Electronic supplementary information

Ligand-free direct heteroarylation approach for benzobithiophenedione-based simple small molecular acceptor toward high efficiency polymer solar cells

Zhuhao Wu[†], Yinchu Chen[†], Lianjie Zhang*, Dong Yuan, Rihang Qiu, Suinan Deng, Haizhen Liu, Zesheng Zhang and Junwu Chen*

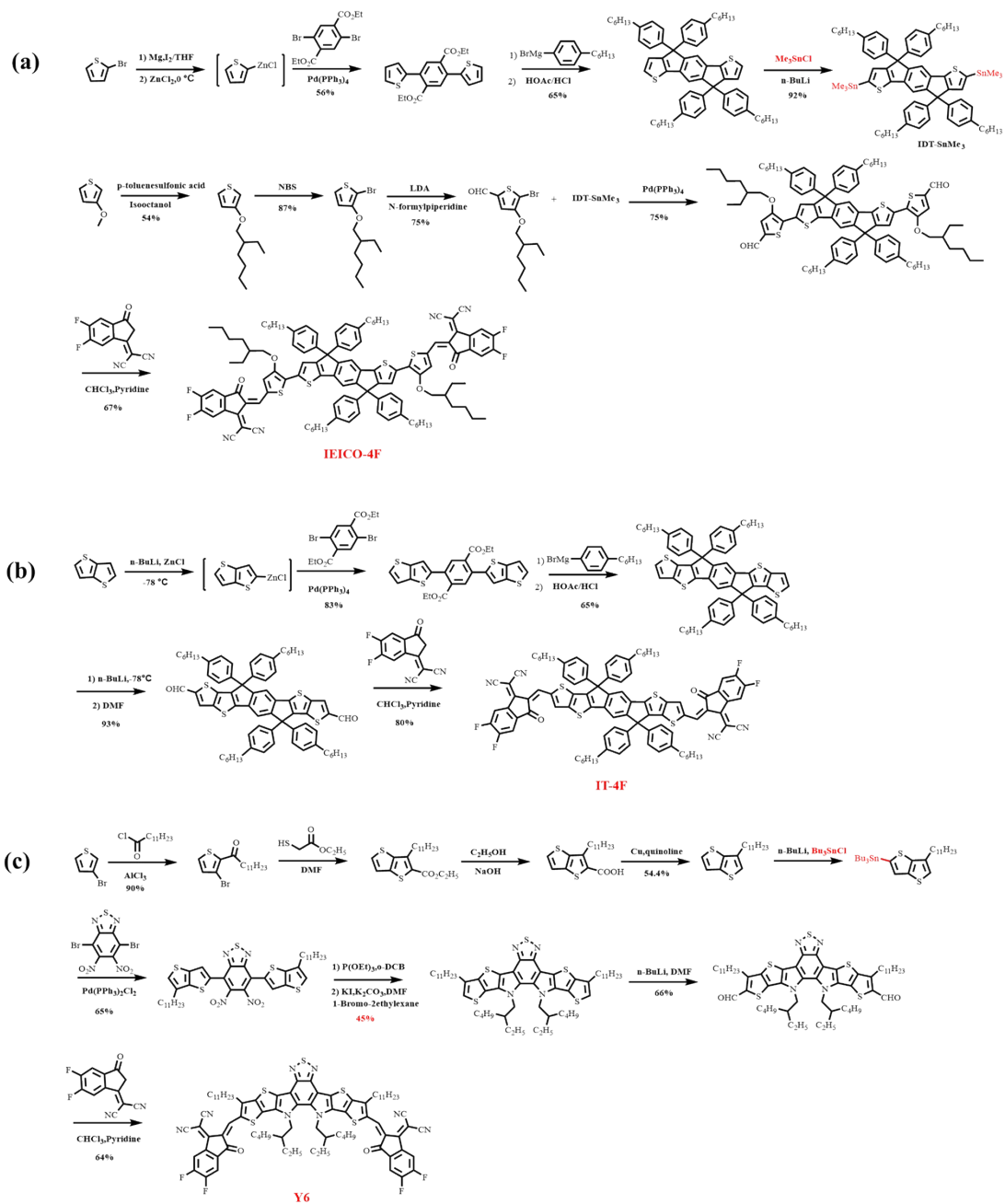Institute of Polymer Optoelectronic Materials & Devices

State Key Laboratory of Luminescent Materials & Devices
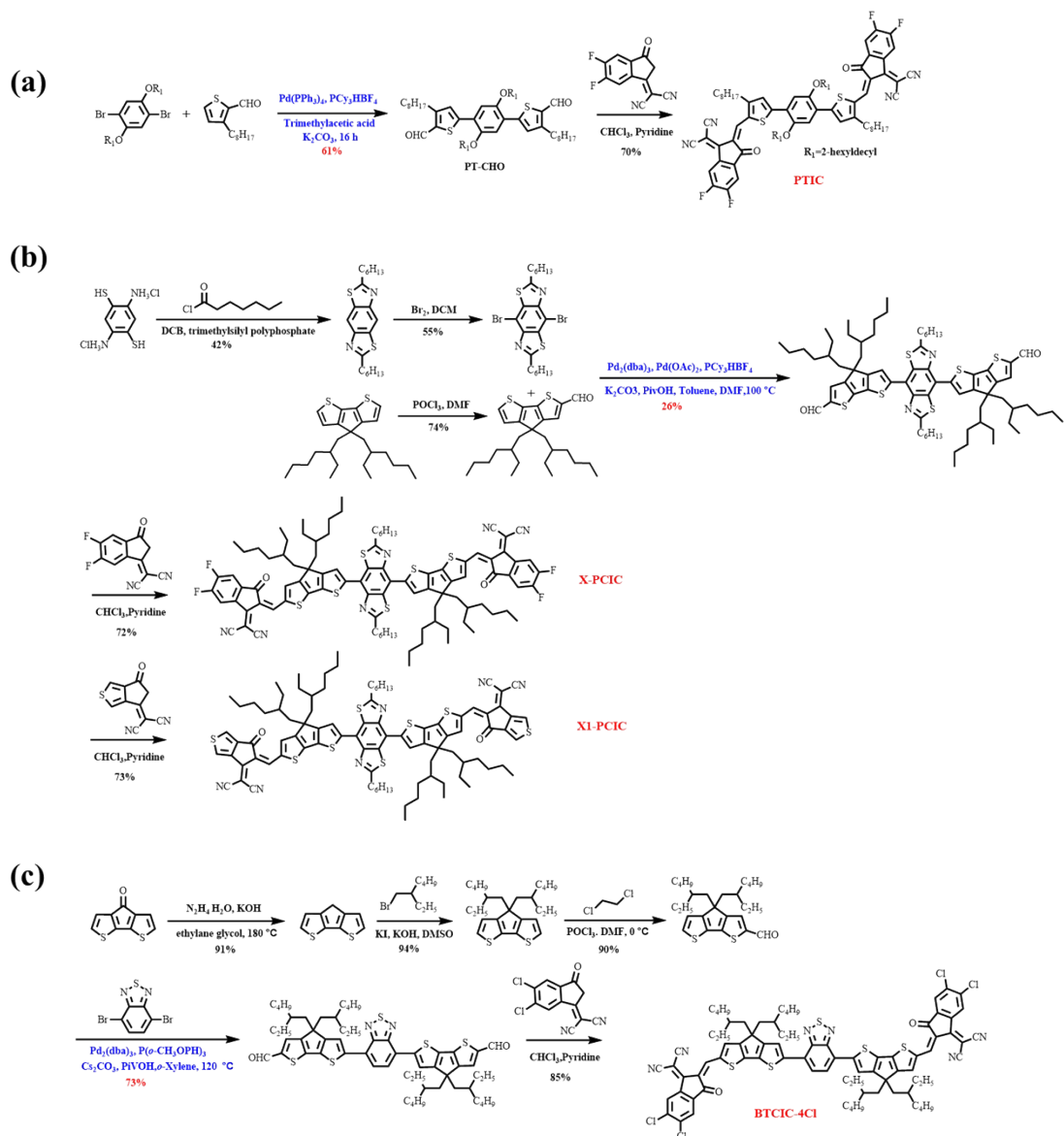
South China University of Technology

Guangzhou 510640, P. R. China

E-mails: lianjiezhang@scut.edu.cn; psjwchen@scut.edu.cn

[†] These authors contributed equally to this article.

Fig. S1 Synthesis routes of a few representative fused-ring electron acceptors: (a) IEICO-4F[1-3], (b) IT-4F[4, 5], and (c) Y6[6].

Fig. S2 Synthesis routes of some simple fused-ring acceptors PTIC (a), X-PCIC and X1-PCIC (b), and BTCIC-4Cl (c) with PCE over 10%, where ligands are employed in the direct C−H arylations.

Table S1. Summary for Reaction condition and PCE of the PSCs based on SFAs

Acceptor	Organotin free	Ligand free	Donor	PCE_{best}	Reference
BDDEH-4F	√	√	PM6	12.59%	This work
BDDBO-4F	√	√	PM6	9.80%	This work
PTIC	√	×	PBDB-TF	10.27%	7
X-PCIC	√	×	PBDB-T	11.33%	8
X1-PCIC	√	×	PBDB-T	10.05%	8
BTCIC-4Cl	√	×	PBDB-T-2Cl	10.50%	9
TPDCIC	×	√	PBDB-T	10.12%	10
DOC2C6-2F	×	√	PBDB-T	13.24%	11
BCDT-4Cl	×	√	PBDB-T	12.10%	12
SiOC2C6-4Cl	×	√	PBDB-T	11.29%	13
o-DOC6-2F	×	√	PBDB-T	11.87%	14
o-DOC8-2F	×	√	PBDB-T	11.23%	14
o-DOC2C6-2F	×	√	PBDB-T	10.80%	14
FOC6-IC	×	√	PBDB-T	10.80%	15
FOC6-FIC	×	√	PBDB-T	12.08%	15
FOC2C6-2FIC	×	√	PBDB-T	12.36%	15
DF-PCIC	×	√	PBDB-T	10.12%	16
HF-PCIC	×	√	PM6	12.59%	17
BTOR-IC4F	×	√	PM6	9.80%	18
o-4TBC-2F	×	√	PBDB-TF	10.27%	19
BTzO-4F	×	√	PBDB-T	13.80%	20

Experimental Section

Synthesis Procedures

All reagents and solvents were purchased from commercial sources (like J&K, Energy Chemical, Derthon and Acros) used without further purification unless otherwise specified. The monomers BDDEH-Br and BDDBO-4Br are commercial, which can purchase from Derthon. All manipulations involving air-sensitive reagents were performed under an atmosphere of dry argon.
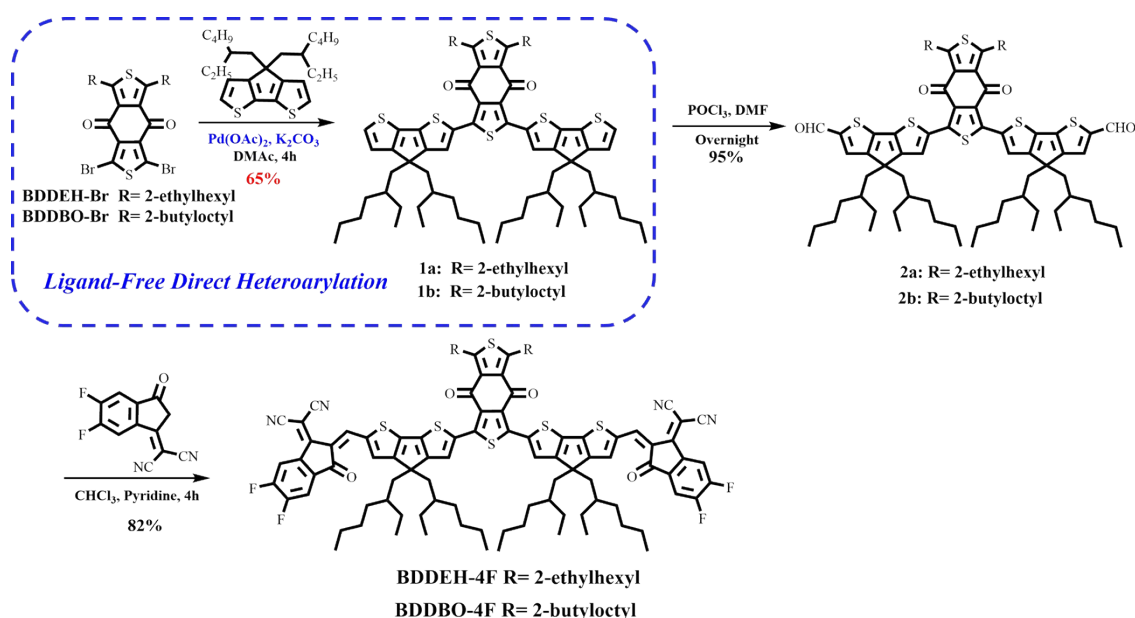
Synthesis of compound 1a

In a 50 mL two-necked flask, 1,3-Dibromo-5,7-bis(2-ethylhexyl)benzo[1,2-c:4,5-c']-dithiophene-4,8-dione (BDDEH-Br) (487.99 mg, 0.8 mmol), 4,4-di(2-ethylhexyl)-cyclopenta [2,1-b:3,4-b']dithiophene (CPDT) (966.48 mg, 2.40 mmol), K_2CO_3 (276.41 mg, 2.00 mmol), Pd(OAc)$_2$ (17.96 mg, 0.08 mmol) were dissolved in N,N-Dimethylacetamide (DMAc) (25 mL) under N_2. Then the mixture was heated up to 80 °C for 4 h, After cooled down to room temperature, water were added, the mixture was

extracted by ethyl acetate three times and washed with water. After the combined organic phase was concentrated, the residue was purified by silica gel column chromatography using petroleum as eluent. The pure compound 1a was obtained as a red brown oil (648 mg, 65%). ^{1}H NMR (400 MHz, CDCl$_3$) δ (ppm): 7.70 (m, 2H), 7.24 (d, J = 4.9 Hz, 2H), 7.03 – 6.87 (m, 2H), 3.50 – 3.23 (m, 4H), 2.04 – 1.84 (m, 10H), 1.43 – 1.20 (m, 18H), 1.18 – 0.77 (m, 40H), 0.82 – 0.50 (m, 30H). ^{13}C NMR (101 MHz, CDCl^3) δ (ppm):177.85, 159.12, 157.37, 152.83, 142.98, 136.89, 133.22, 132.90, 132.86, 131.03, 126.38, 125.51, 122.40, 53.66, 43.24, 41.42, 35.15, 35.09, 34.28, 34.22, 33.64, 32.86, 28.95, 28.61, 27.38, 26.93, 26.05, 23.08, 22.89, 22.87, 22.79, 14.26, 14.19, 14.10, 10.94, 10.75, 10.63, 10.61. MS (MALDI-TOF): *m/z* 1245.62 (M$^+$).

Synthesis of compound 1b

The synthesis steps of compound 1b are similar to that of compound 1a. Compound 1b was obtained as a red brown oil (717.17 mg, 66%).^{1}H NMR (500 MHz, CDCl$_3$) δ (ppm): 7.71 – 7.65 (m, 2H), 7.24 (d, J = 4.8 Hz, 2H), 6.97 (dt, J = 5.0, 2.6 Hz, 2H), 3.45 – 3.30 (m, 4H), 1.99 – 1.82 (m, 10H), 1.40 – 1.25 (m, 30H), 1.06 – 0.84 (m, 44H), 0.79 – 0.71 (m, 12H), 0.71 – 0.57 (m, 18H). ^{13}C NMR (126 MHz, CDCl^3) δ (ppm): 177.84, 159.26, 157.19, 152.81, 143.00, 136.91, 133.17, 132.89, 130.96, 130.85, 126.37, 125.46, 122.39, 53.65, 43.22, 39.94, 35.13, 35.07, 34.26, 34.21, 34.04, 33.73, 33.44, 31.87, 29.70, 28.92, 28.59, 27.48, 27.36, 26.63, 23.08, 22.88, 22.85, 22.78, 22.70, 14.26, 14.18, 14.12, 14.09, 10.72, 10.61, 10.59. MS (MALDI-TOF): *m/z* 1359.74 (M$^+$).

Synthesis of compound 2a

In a 50 mL two-necked flask, the compound 1a (361.36 mg, 0.29 mmol) was dissolved in DMF (25 mL) under an argon atmosphere, $POCl_3$ (1.33 g, 8.70 mmol) was added dropwise into the mixture solution at 0 ℃. After being stirred at 0 ℃ for 2 h, then the mixture was heated up to 80 °C overnight. After reaction finished, the mixture was pour into cold NaOH aqueous solution. The crude product was extracted with ethyl acetate and washed with NaCl aqueous solution. After removing the solvent, silica gel column chromatography was used to purify the product with the mixture of petroleum ether and dichloromethane (1:1,v/v) as the eluent. The pure compound 3 was obtained as red oil (360 mg, 95%). ^1H NMR (500 MHz, $CDCl_3$) δ (ppm): 9.87 (s, 2H), 7.73 – 7.70 (m, 2H), 7.60 (t, J = 4.4 Hz, 2H), 3.43 – 3.31 (m, 4H), 2.03 – 1.93 (m, 8H), 1.79 (s, 2H), 1.45 – 1.25 (m, 18H), 1.04 – 0.89 (m, 40H), 0.81 – 0.71 (m, 12H), 0.72 – 0.59 (m, 18H). ^{13}C NMR (126 MHz, $CDCl_3$) δ (ppm): 182.63, 177.68, 161.09, 158.68, 153.92, 147.31, 144.36, 142.46, 140.94, 137.21, 132.81, 132.50, 130.49, 125.35, 54.17, 43.14, 41.39, 35.31, 35.25, 34.39, 34.19, 33.68, 32.81, 31.51, 29.70, 28.90, 28.56, 27.59, 27.35, 26.92, 26.02, 23.04, 22.76, 14.26, 14.14, 14.07, 10.89, 10.68, 10.60.

Synthesis of compound 2b

The synthesis steps of compound 2b are similar to that of compound 2a. Compound 2b was obtained as a red oil (540 mg, 96%). ^1H NMR (400 MHz, $CDCl_3$) δ (ppm): 9.87 (s, 2H), 7.71 (dt, J = 5.6, 2.8 Hz, 2H), 7.60 (t, J = 3.5 Hz, 2H), 3.46 – 3.24 (m, 4H), 2.07 – 1.91 (m, 8H), 1.84 (s, 2H), 1.45 – 1.21 (m, 30H), 1.09 – 0.83 (m, 44H), 0.80 – 0.71

(m, 12H), 0.69-0.6 (m, 18H). ^{13}C NMR (101 MHz, CDCl$_3$) δ (ppm): 182.63, 177.63, 161.03, 160.96, 158.68, 153.93, 147.32, 144.38, 142.47, 140.98, 137.22, 132.80, 130.50, 125.32, 54.17, 43.15, 39.95, 35.32, 35.26, 34.44, 34.38, 34.20, 34.12, 33.70, 33.42, 31.92, 29.68, 28.89, 28.56, 27.61, 27.54, 27.35, 26.59, 23.07, 22.85, 22.77, 22.70, 14.28, 14.13, 14.08, 10.71, 10.62, 10.61.

Synthesis of BDDEH-4F

In 50 mL two-necked flask, the compound 2a (260.42 mg, 0.20 mmol), (2-(5,6-difluoro-3-oxo-2,3-dihydro-1H-inden-1-ylidene)malononitrile (138.10 mg, 0.60 mmol) and pyridine (0.1 mL) were dissolved in chloroform (25 mL). Then the mixture was heated at 60°C and stirred for 4h. After cooling to room temperature, the mixture was poured into methanol (150 mL) and filtered. The residue was purified by silica gel column chromatography using dichloromethane/petroleum ether (1/1, v/v) as the eluent to give a dark blue solid (283.84 mg, 82%). ^{1}H NMR (500 MHz, CDCl$_3$) δ (ppm): 8.92 (s, 2H), 8.54 (dd, J = 9.8, 6.5 Hz, 2H), 7.77 (t, J = 5.8 Hz, 2H), 7.69 (t, J = 7.4 Hz, 4H), 3.45 – 3.33 (m, 4H), 2.08 – 1.97 (m, 8H), 1.82 (s, 2H), 1.49 – 1.32 (m, 16H), 1.07 – 0.92 (m, 44H), 0.78 – 0.71 (m, 16H), 0.69 – 0.64 (m, 12H). ^{13}C NMR (126 MHz, CDCl$_3$) δ (ppm): 186.06, 177.48, 164.18, 160.19, 158.47, 157.78, 155.32, 154.53, 153.33, 142.31, 141.46, 140.74, 139.82, 138.17, 136.54, 134.49, 133.46, 132.59, 125.55, 120.13, 115.00, 114.82, 114.59, 112.60, 112.45, 68.54, 54.13, 43.17, 41.36, 35.47, 34.35, 34.30, 34.10, 33.76, 32.70, 28.83, 28.54, 28.47, 27.57, 27.51, 27.34, 25.96, 23.06, 22.87, 22.84, 22.81, 14.26, 14.16, 14.10, 10.87, 10.63. MS (MALDI-TOF): m/z 1725.67 (M$^+$).

Synthesis of BDDBO-4F

The synthesis steps of BDDBO-4F are similar to that of BDDEH-4F. BDDBO-4F was obtained as a red oil (157.59 mg, 83%). ^{1}H NMR (500 MHz, CDCl$_3$) δ (ppm): 8.92 (s, 2H), 8.54 (dd, J = 9.8, 6.5 Hz, 2H), 7.77 (dd, J = 7.9, 3.8 Hz, 2H), 7.75 – 7.64 (m, 4H), 3.47 – 3.31 (m, 4H), 2.09 – 1.98 (m, 8H), 1.87 (s, 2H), 1.44 – 1.27 (m, 32H), 1.06 – 0.86 (m, 44H), 0.79 – 0.71(m, 16H), 0.69 – 0.64 (m, 12H). ^{13}C NMR (126 MHz, CDCl$_3$) δ (ppm): 186.02, 177.47, 164.14, 160.19, 158.47, 157.78, 155.32, 154.58, 153.33, 153.22, 153.22, 142.31, 141.50, 140.72, 139.84, 138.15, 136.54, 134.50, 133.44, 132.59, 125.49, 120.14, 114.99, 114.59, 112.60, 68.52, 54.14, 43.28, 43.17, 39.98, 35.47, 34.36, 34.31, 34.19, 34.11, 33.62, 33.32, 31.93, 29.70, 28.82, 28.54, 28.48, 27.58, 27.51, 27.34, 26.56, 23.08, 22.87, 22.85, 22.81, 22.71, 14.28, 14.14, 14.10, 10.63. MS (MALDI-TOF): m/z 1837.80 (M$^+$).
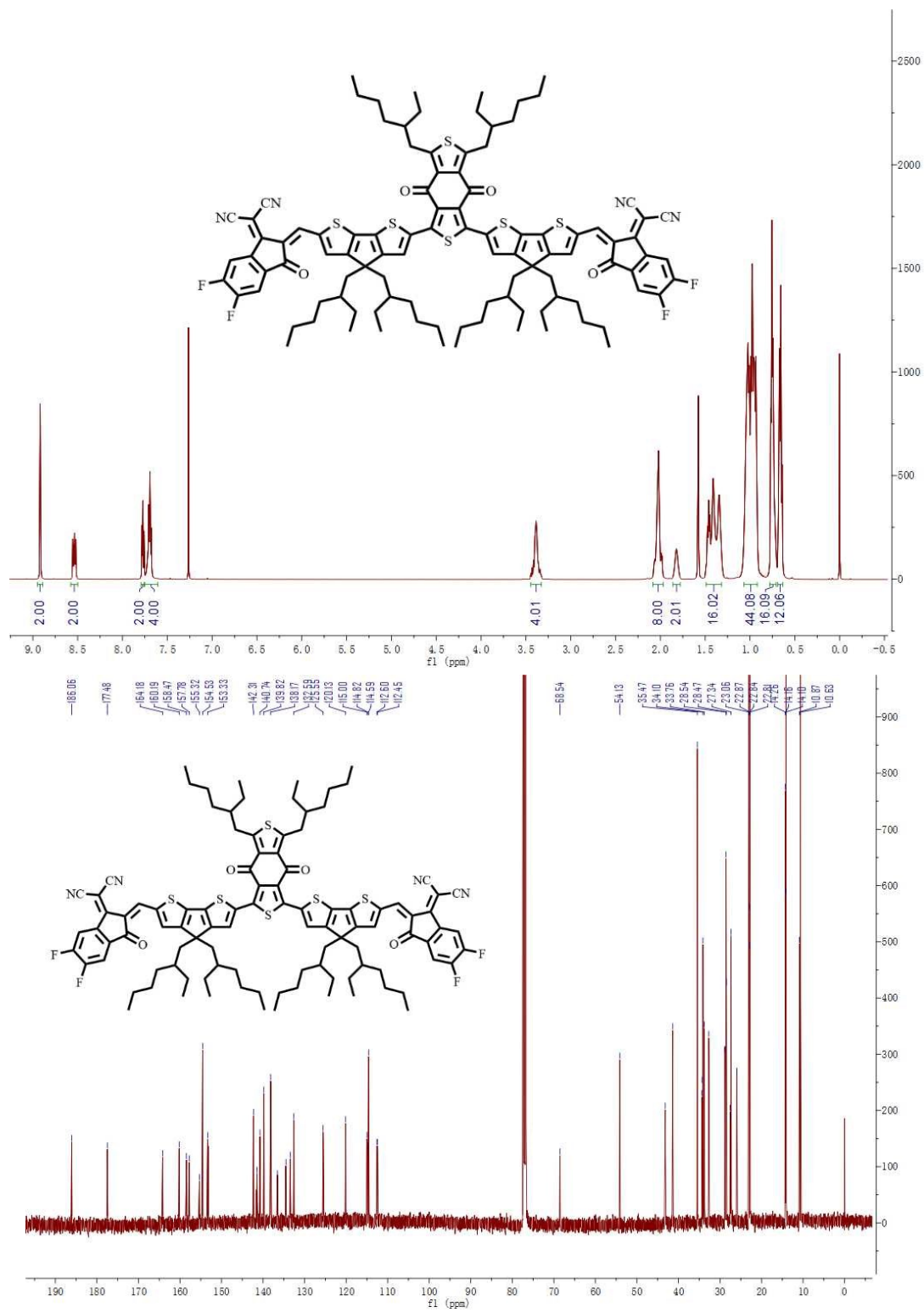
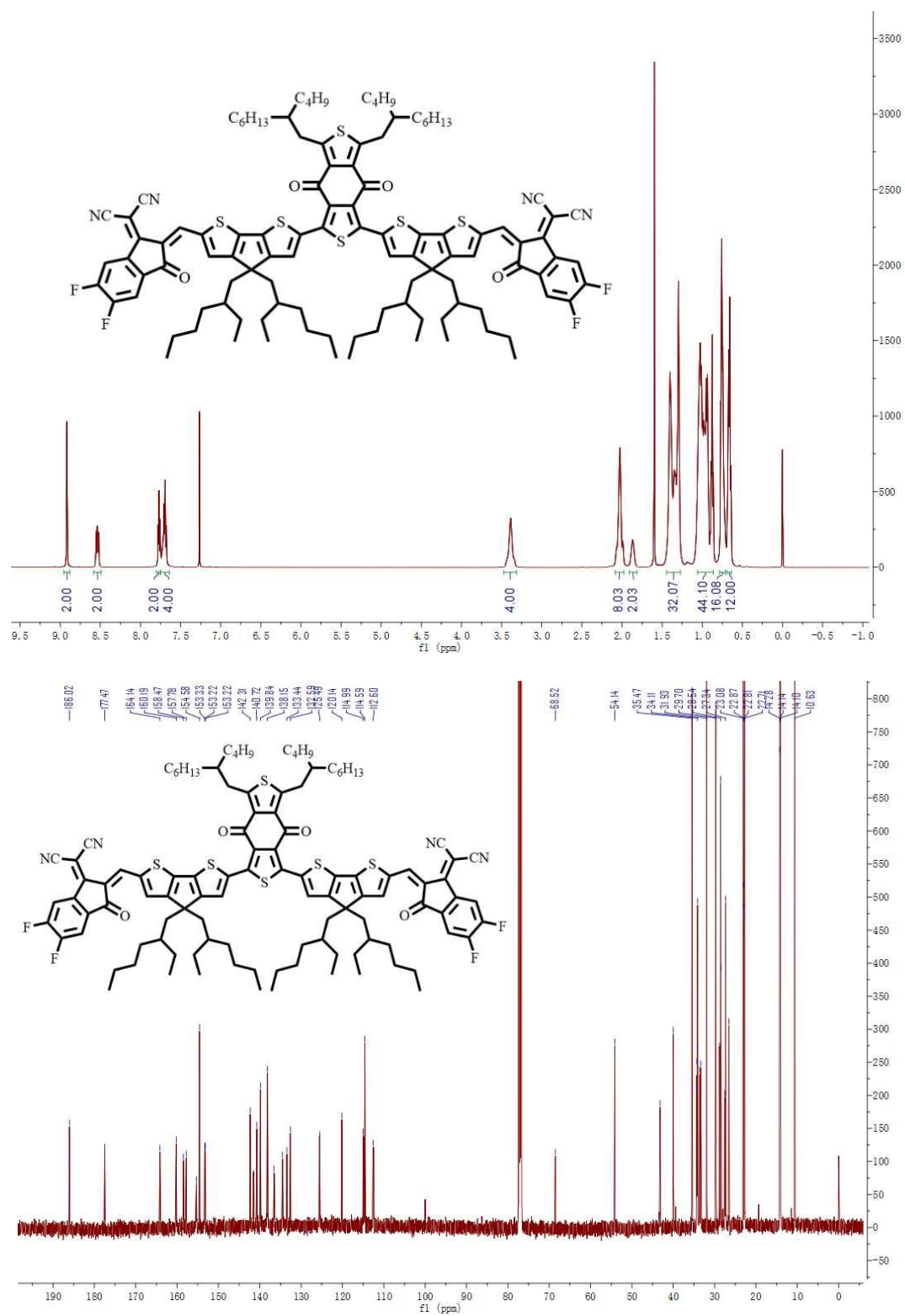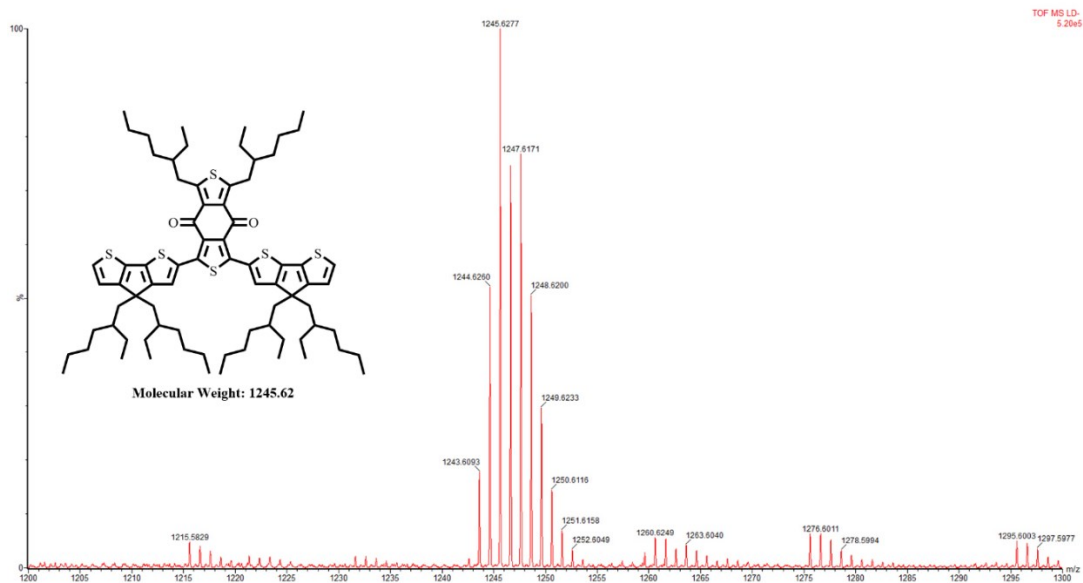**Fig. S3** ^{1}H NMR and ^{13}C NMR spectrum of **BDDEH-4F**

S10

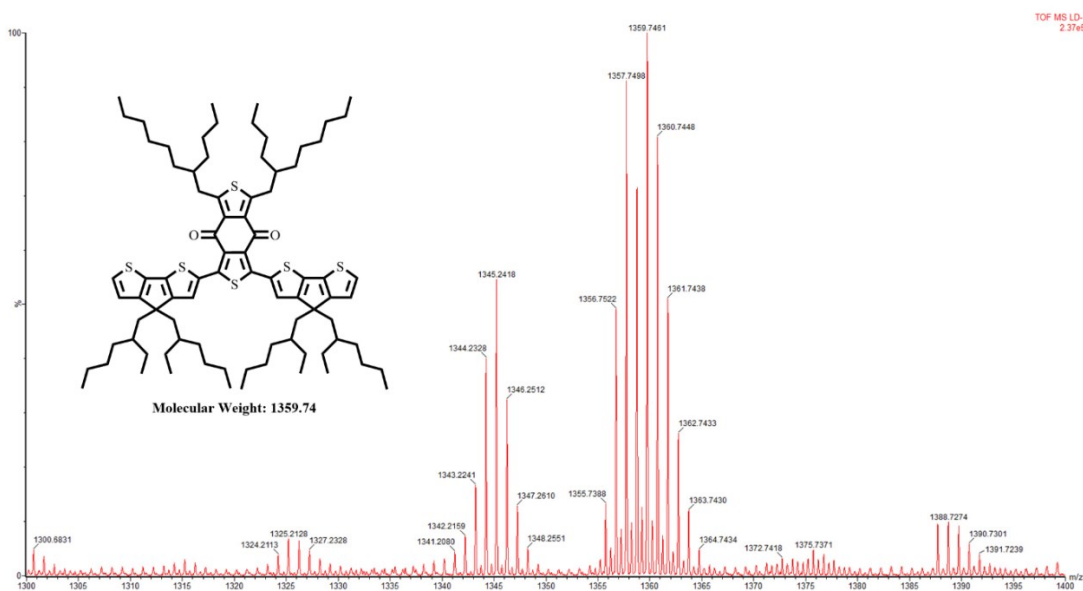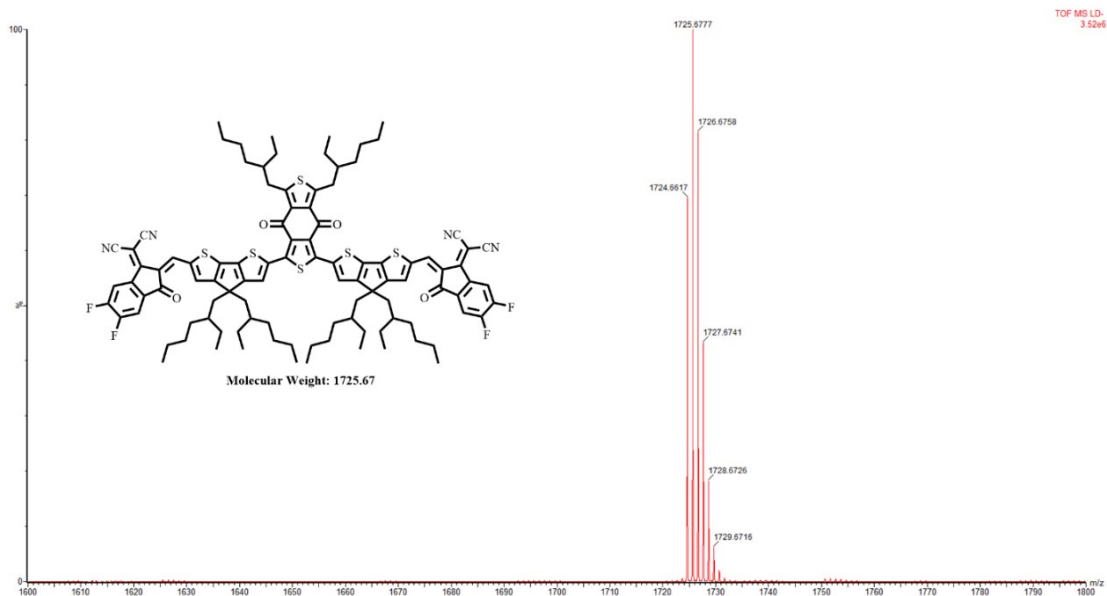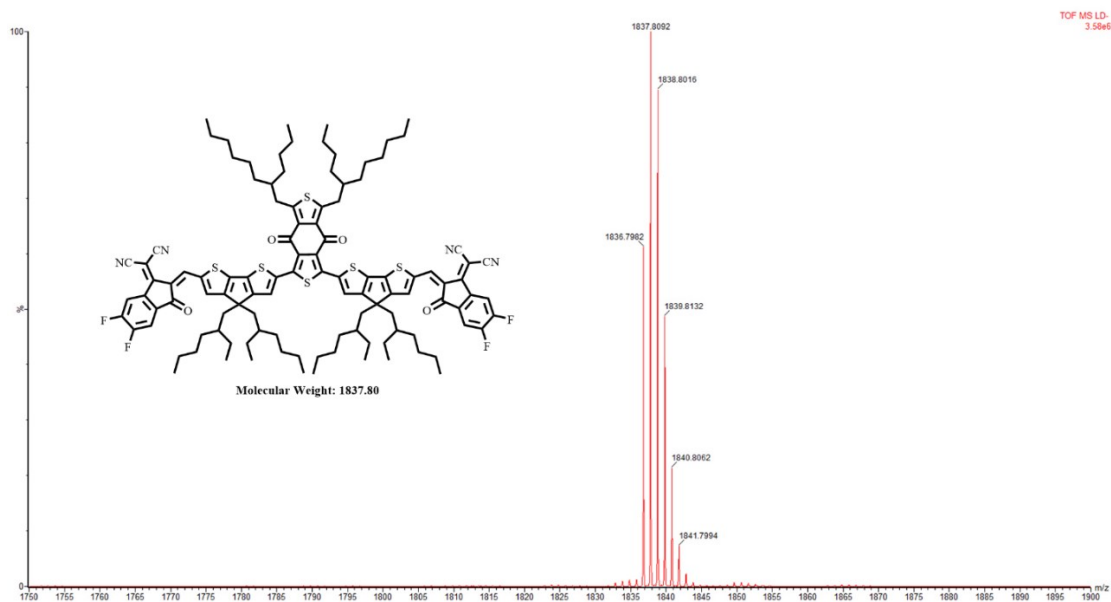**Fig. S4** ^{1}H NMR and ^{13}C NMR spectrum of **BDDBO-4F**

Fig. S5 The MALDI-TOF MS plot of **compound 1a**
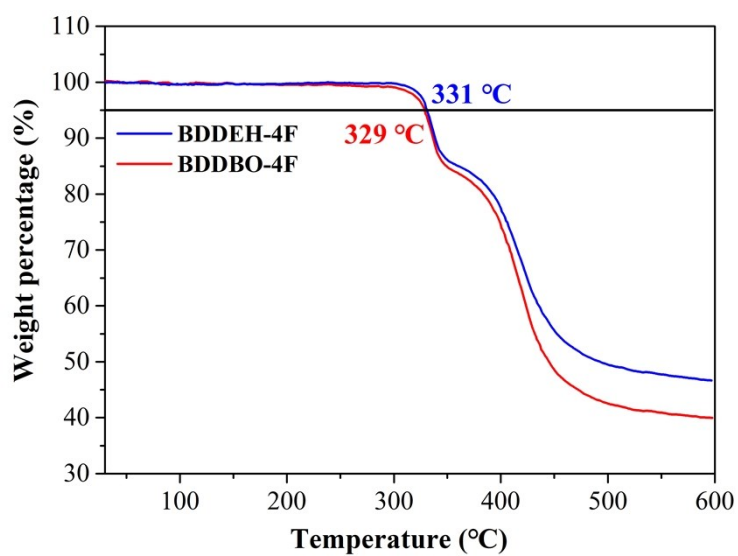

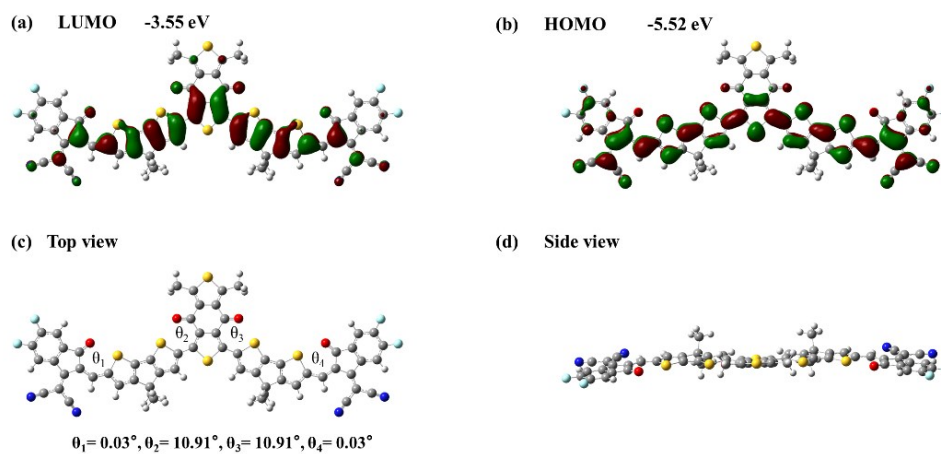**Fig. S6** The MALDI-TOF MS plot of **compound 1b**

Fig. S7 The MALDI-TOF MS plot of **BDDEH-4F**

Fig. S8 The MALDI-TOF MS plot of **BDDBO-4F**
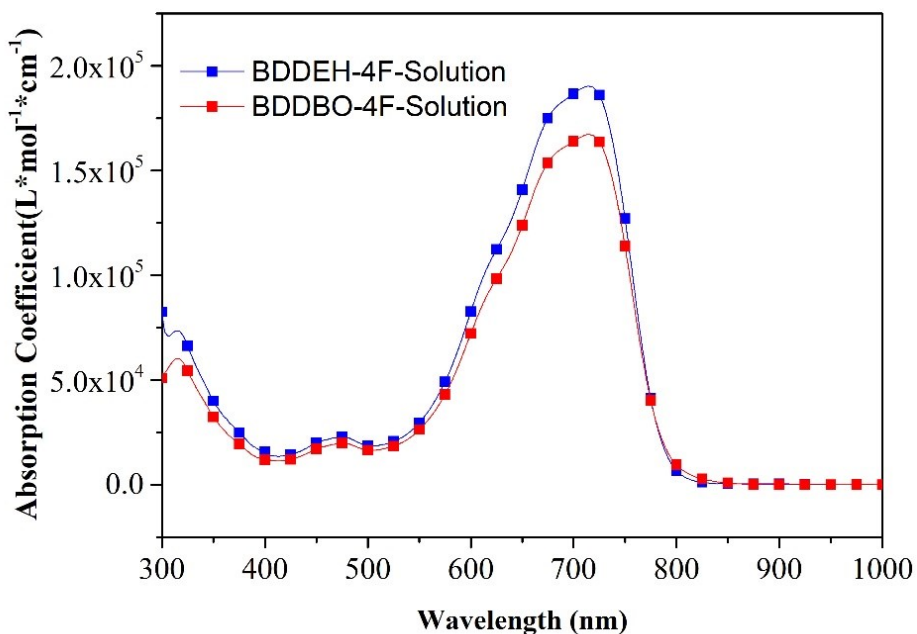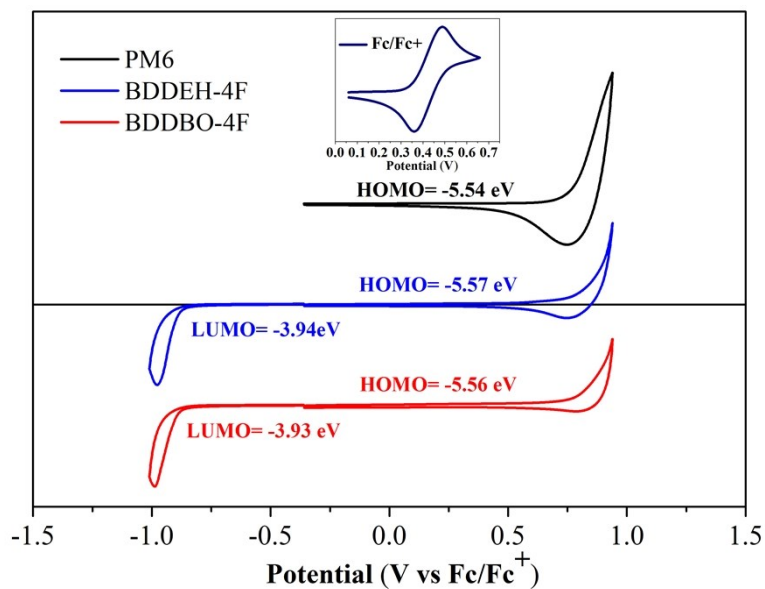
S13

Fig. S9 TGA image of BDDEH-4F and BDDBO-4F under N_2 atmosphere.

Fig. S10 The optimized frontier molecular orbitals and conformations obtained by DFT calculations for BDD core based acceptors.

Fig. S11 Absorption coefficients of BDDEH-4F and BDDBO-4F in chloroform solutions.

Fig. S12 Cyclic voltammetry measurements of BDDEH-4F and BDDBO-4F.

Table S2. Optical and electrochemical properties of BDDEH-4F and BDDBO-4F

Acceptor	λ_{max} (nm)		λ_{onset}	ε_{max}	Eg^{opt}	HOMO	LUMO	E_g^{cv}
	Solution	Film	(nm)	$(M^{-1}\ cm^{-1})$	(eV)	(eV)	(eV)	(eV)
BDDEH-4F	715	776	877	1.90×10^5	1.41	−5.57	−3.94	1.63
BDDBO-4F	714	773	873	1.67×10^5	1.42	−5.56	−3.93	1.63

Device Fabrication and Characterization

The device structure was ITO/ZnO/Donor:Acceptor/MoO$_3$/Al. Patterned indium tin oxide (ITO)-coated glass with a sheet resistance of 15–20 ohm/square was cleaned by a surfactant scrub and then underwent a wet-cleaning process inside an ultrasonic bath that began with deionized water, followed by acetone and 2-propanol. A solution-processed zinc oxide (ZnO) interlayer of 30 nm was prepared according to a recent report.[21] The substrates were then transferred into a nitrogen-filled glove box.Active layer solutions with PM6 and acceptor (BDDEH-4F or BDDBO-4F) were prepared in CB solvent. The solutions were then spin-coated onto the substrates and dried under vacuum. A 10 nm MoO$_3$ layer and a 100 nm Al layer were subsequently evaporated through a shadow mask to define the active area of the devices (5.8 mm^2) and form the top anode.

The PCE was determined from *J-V* curve measurements (using a Keithley 2400 sourcemeter) under a 1 sun, AM 1.5G spectrum from a solar simulator (Oriel model 91192; 1000 W m^{-2}). All the masked and unmasked tests gave consistent results with relative errors within 5%. The solar simulator illumination intensity was determined using a monocrystal silicon reference cell (Enli/SRC2020, with KG-5 visible color filter) calibrated by the National Renewable Energy Laboratory (NREL). Theoretical

J_{sc} values obtained by integrating the product of the EQE with the AM 1.5G solar spectrum agreed with the measured value to within 5%.

Table S3. Photovoltaic performance of PSCs based on PM6:BDDEH-4F with different D:A ratio

Donor:Acceptor	D:A	V_{oc} (V)	J_{sc} (mA·cm^{-2})	FF (%)	PCE (%)
PM6:BDDEH-4F	1:1	0.89	18.58	50.67	8.39
	1:1.2	0.89	18.96	49.12	8.30
	1:1.5	0.88	17.59	47.51	7.36

Table S4. Photovoltaic performance of PSCs based on PM6:BDDEH-4F, with different annealing temperature and annealing time.

Donor:Acceptor	Annealing Temperature	V_{oc} (V)	J_{sc} (mA·cm^{-2})	FF (%)	PCE (%)
PM6:BDDEH-4F (1:1)	as cast	0.89	18.58	50.67	8.39
	90 °C+10 min	0.89	20.43	51.18	8.67
	120 °C+10 min	0.87	20.49	55.36	9.88
	160 °C+5 min	0.86	21.78	60.9	11.42
	160 °C+10 min	0.88	21.63	62.60	11.93
	160 °C+15 min	0.86	22.76	58.07	11.38
	180 °C+10 min	0.85	21.26	57.98	11.16
PM6:BDDEH-4F (1:1.2)	as cast	0.89	18.96	49.12	8.30
	120 °C+10 min	0.88	20.44	52.43	9.44
	140 °C+10 min	0.87	21.48	56.94	10.65
	160 °C+10 min	0.87	22.36	58.43	11.38
PM6:BDDEH-4F (1:1.5)	as cast	0.88	17.59	47.51	7.36
	120 °C+10 min	0.88	21.29	52.03	9.09
	140 °C+10 min	0.88	21.42	55.79	10.53
	160 °C+10 min	0.87	22.46	56.82	11.11

Table S5. Varied amount of 1-chloronaphthalene (CN) of PSCs devices based BDDEH-4F with different D:A ratio and annealing temperature of 160 °C and annealing time of 10 min.

Donor:Acceptor	CN (vol%)	V_{oc} (V)	J_{sc} (mA·cm^{-2})	FF (%)	PCE (%)
PM6:BDDEH-4F (1:1)	0	0.88	21.63	62.60	11.93
	0.5%	0.88	22.57	63.38	12.59
	1.0%	0.87	20.03	64.35	11.23
	1.5%	0.86	19.79	64.95	11.07
PM6:BDDEH-4F (1:1.2)	0	0.87	22.36	58.43	11.38
	0.5%	0.85	21.97	58.43	10.93
	1.0%	0.86	20.75	63.25	11.30
	1.5%	0.86	20.16	63.10	10.83
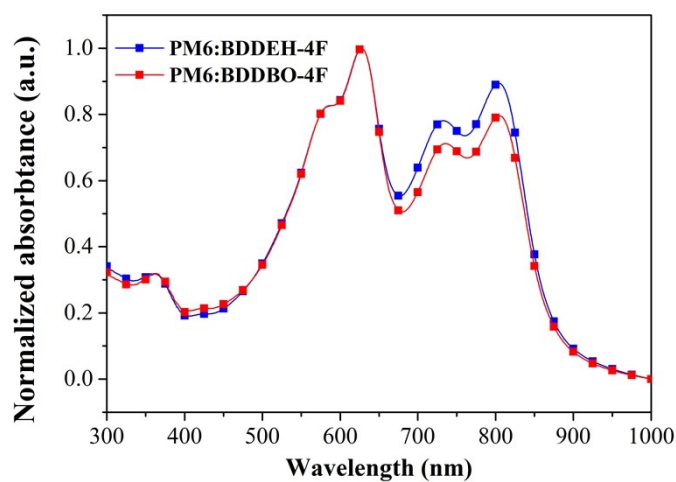
Fig. S13 Normalized thin film UV-vis absorption spectra of PM6:BDDEH-4F and PM6:BDDBO-4F under optimized condition.
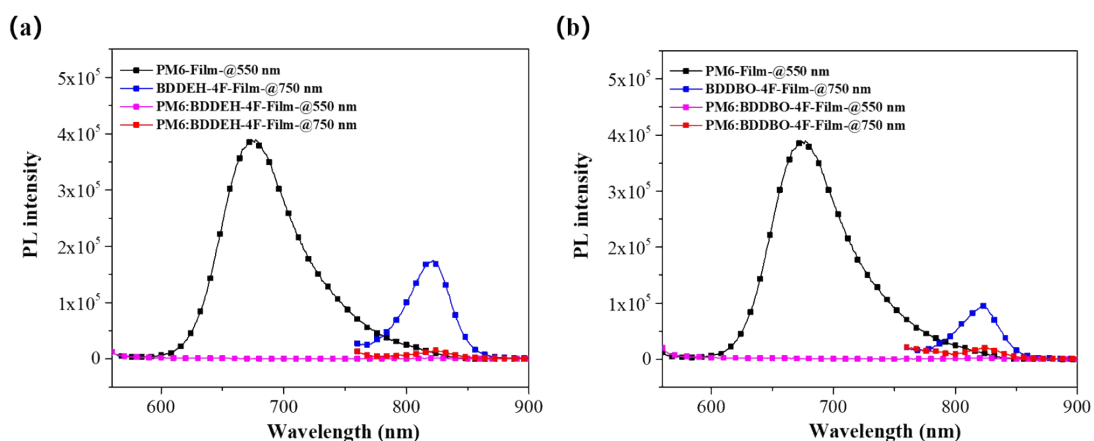
Fig. S14 PL spectra of the neat films and optimized PM6:BDDEH-4F (a) and PM6:BDDBO-4F (b) blend films. Polymer PM6 and acceptors are excited at 550 and 750 nm, respectively.
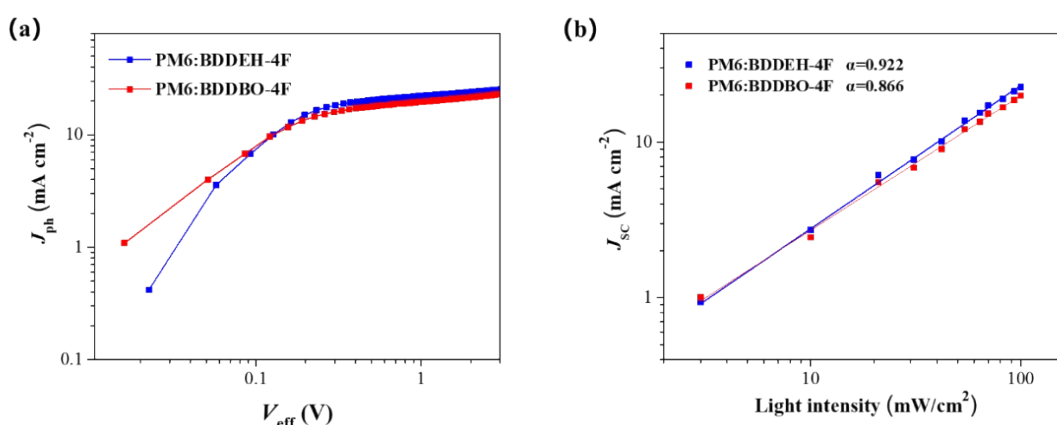
Fig. S15 Photocurrent density versus effective voltage (a) and dependence of J_{sc} on light intensity (b) for the optimized PM6:BDDEH-4F and PM6:BDDBO-4F based devices.

Space-Charge Limited Current (SCLC) Measurement.

Hole-only and electron-only devices were fabricated to measure the hole and electron mobilities of active layers using the space charge limited current (SCLC) method with hole-only device of ITO/PEDOT:PSS/Active layer/MoO₃/Al and electron-only device

of ITO/ZnO/Active layer/PFN-Br/Al. The mobilities (μ) were determined by fitting the

dark current to the model of a single carrier SCLC, described by the equation:

$$J = \frac{9}{8}\varepsilon_0\varepsilon_r\mu\frac{V^2}{d^3}$$

where J is the current, ε_0 is the permittivity of free space, ε_r is the material relative

permittivity, d is the thickness of the active layer, and V is the effective voltage. The

effective voltage can be obtained by subtracting the built-in voltage (V_{bi}) and the

voltage drop (V_s) from the substrate's series resistance from the applied voltage (V_{appl}),

$V = V_{appl} - V_{bi} - V_s$. The mobility can be calculated from the slope of the $J^{1/2} \sim V$ curves.
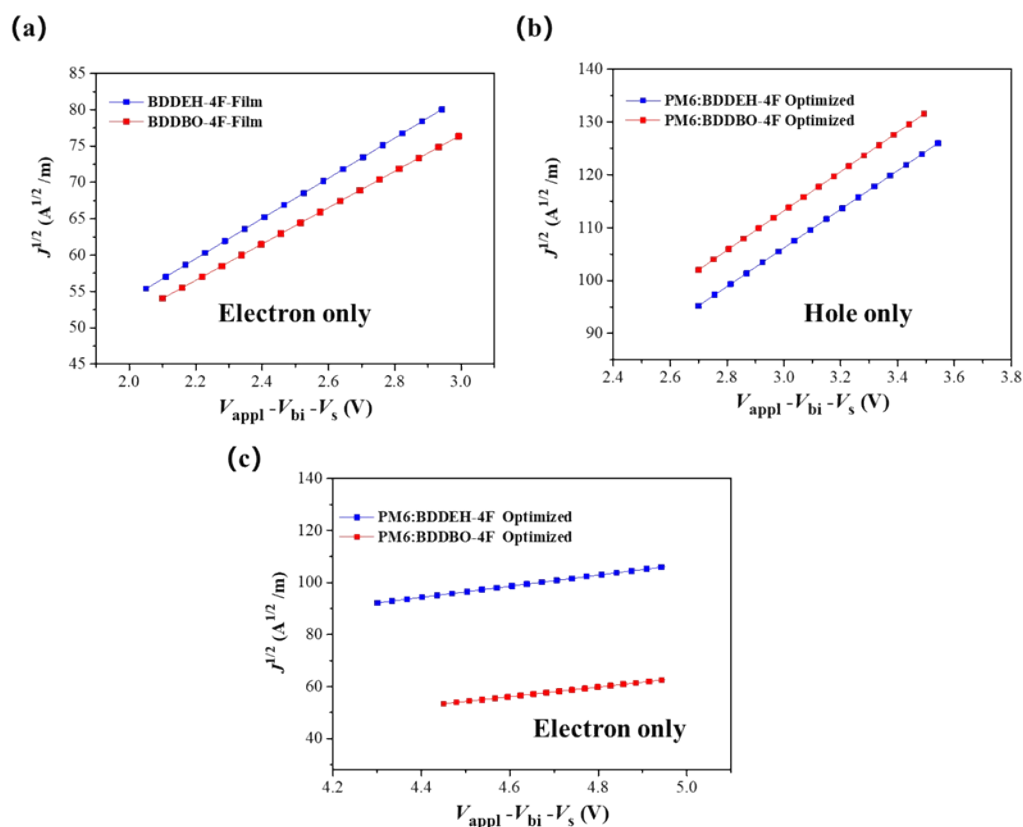
Fig. S16 SCLC $J^{1/2}$-V characteristics of the PM6:acceptors blend films in (a) hole-only

and (b) electron-only devices, with device configurations of ITO/ PEDOT:PSS/ blend

film/MoO$_3$/Al and ITO/ZnO/blend film/PFN-Br/Al, respectively.

Contact angle measurements.

The contact angle tests were performed on a Dataphysics OCA40 Micro surface contact angle analyzer. The surface energy of the polymers and acceptors were characterized and calculated by the contact angles of the two probe liquids (water and diiodomethane) using the Wu model.[22]

$$\frac{4\gamma_{water}^{d}\gamma_{s}^{d}}{\gamma_{water}^{d}+\gamma_{s}^{d}} + \frac{4\gamma_{water}^{p}\gamma_{s}^{p}}{\gamma_{water}^{p}+\gamma_{s}^{p}} = \gamma_{water}(1+\cos\theta_{water})$$

$$\frac{4\gamma_{oil}^{d}\gamma_{s}^{d}}{\gamma_{oil}^{d}+\gamma_{s}^{d}} + \frac{4\gamma_{oil}^{p}\gamma_{s}^{p}}{\gamma_{oil}^{p}+\gamma_{s}^{p}} = \gamma_{oil}(1+\cos\theta_{oil})$$

$$\gamma_{s}=\gamma_{s}^{d}+\gamma_{s}^{p}$$

where γ_{s} is the total surface tension of acceptors and polymers, γ_{s}^{d} and γ_{s}^{p} are the dispersion and polar components of γ_{s}, the values of γ_{water}^{d}, γ_{water}^{p}, γ_{oil}^{d}, γ_{oil}^{p} could be found from the literature and θ is the droplet contact angle between sample and probe liquid.[23]
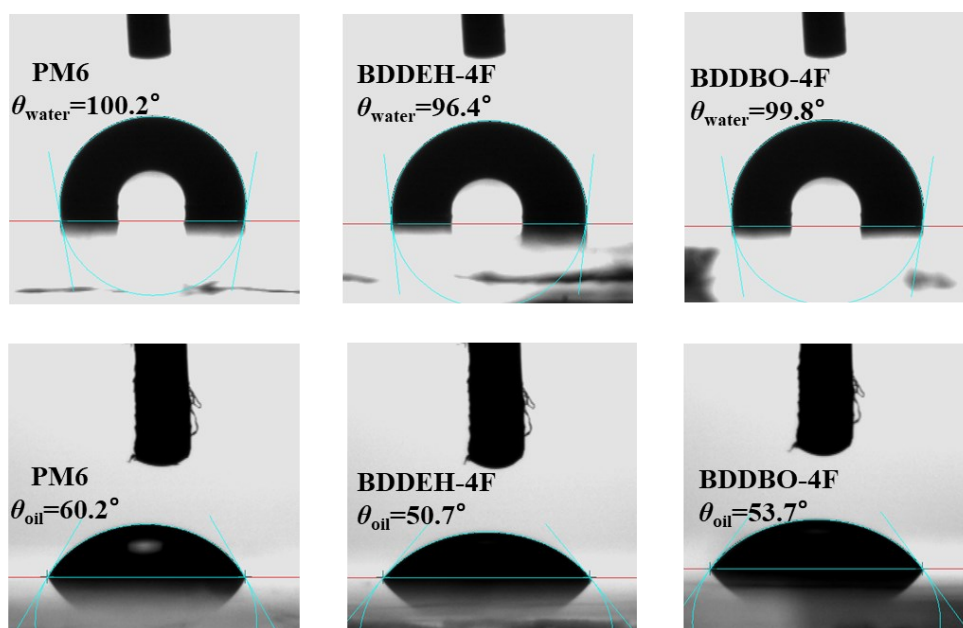
Fig. S17 Views of surface contact measurements for the films of PM6 and acceptors.

**Table S6.** The contact angles and surface energy parameters of the films.

Film	Contact angle		γ^d [mN/m]	γ^p [mN/m]	γ [mN/m]	χ
	θ_{water} (°)	θ_{oil} (°)[a]				
PM6	100.2	60.2	27.95	2.88	30.83	
BDDEH-4F	96.4	50.7	32.29	3.35	35.64	0.174K
BDDBO-4F	99.8	53.7	31.40	2.33	33.73	0.065K

[a] θ_{oil} represents the contact angle of diiodomethane. γ^d and γ^p represent the surface free energy (γ) generated from the dispersion forces and the polar forces, respectively.

Table S7. Structural parameters of PM6, BDDEH-4F and BDDBO-4F films obtained from the GIWAXS.

Film	In plane direction (100) peak		Out of plane direction (010) peak	
	Scattering vector (q) [Å⁻¹]	d-spacing [Å]	Scattering vector (q) [Å⁻¹]	π-π distance [Å]

PM6	0.287	21.85	1.763	3.56
BDDEH-4F	0.364	17.23	1.819	3.45
BDDBO-4F	0.372	16.89	1.760	3.57
PM6:BDDEH-4F	0.309	20.29	1.831	3.43
PM6:BDDBO-4F	0.324	19.37	1.796	3.50
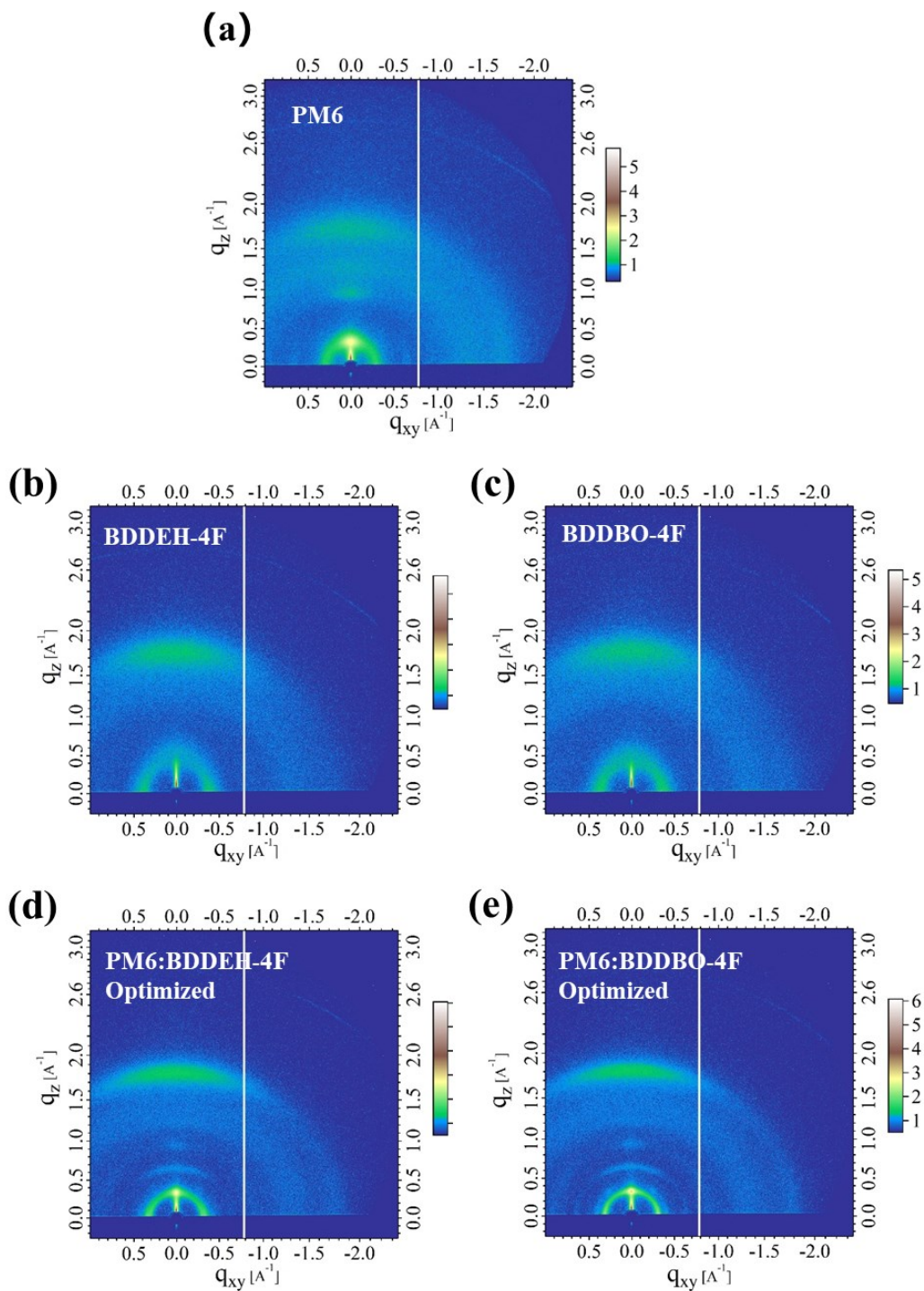
Fig. S18 2D GIWAXS images of films of PM6, BDDEH-4F, BDDBO-4F, PM:BDDEH-4F, and PM6:BDDBO-4F

References

1. H. Yao, Y. Chen, Y. Qin, R. Yu, Y. Cui, B. Yang, S. Li, K. Zhang and J. Hou, *Adv. Mater.*, 2016, **28**, 8283−8287.

2. H. Yao, Y. Cui, R. Yu, B. Gao, H. Zhang and J. Hou, *Angew.Chem. Int. Ed.*, 2017, **56**, 3045−3049.

3. Y. C. Chen, C. Y. Yu, Y. L. Fan, L. I. Hung, C. P. Chen and C. Ting, *Chem. Commun.*, 2010, **46**, 6503−6505.

4. Y. X. Xu, C. C. Chueh, H. L. Yip, F. Z. Ding, Y. X. Li, C. Z. Li, X. Li, W. C. Chen and A. K. Jen, *Adv. Mater.*, 2012, **24**, 6356−6361.

5. W. Zhao, S. Li, H. Yao, S. Zhang, Y. Zhang, B. Yang and J. Hou, *J. Am. Chem. Soc.*, 2017, **139**, 7148−7151.

6. J. Yuan, Y. Zhang, L. Zhou, G. Zhang, H.-L. Yip, T.-K. Lau, X. Lu, C. Zhu, H. Peng, P. A. Johnson, M. Leclerc, Y. Cao, J. Ulanski, Y. Li and Y. Zou, *Joule.*, 2019, **3**, 1140−1151.

7. Z. P. Yu, Z. X. Liu, F. X. Chen, R. Qin, T. K. Lau, J. L. Yin, X. Kong, X. Lu, M. Shi, C. Z. Li and H. Chen, *Nat. Commun.*, 2019, **10**, 2152.

8. S. Li, L. Zhan, T. K. Lau, Z. P. Yu, W. Yang, T. R. Andersen, Z. Fu, C. Z. Li, X. Lu, M. Shi and H. Chen, *Small Methods.*, 2019, **3**, 1900531.

9. S. Pang, X. Zhou, S. Zhang, H. Tang, S. Dhakal, X. Gu, C. Duan, F. Huang and Y. Cao, *ACS Appl. Mater. Interfaces.*, 2020, **12**, 16531−16540.

10. S. Geng, W. Yang, J. Gao, S. Li, M. Shi, T. Lau, X. Lu, C. Li and H. Chen, *Chin. J. Polym Sci.*, 2019, **37**, 1005−1014.

11. H. Huang, Q. Guo, S. Feng, C. Zhang, Z. Bi, W. Xue, J. Yang, J. Song, C. Li, X. Xu, Z. Tang, W. Ma and Z. Bo, *Nat. Commun.*, 2019, **10**, 3038.

12. C. He, Y. Li, S. Li, Z. P. Yu, Y. Li, X. Lu, M. Shi, C. Z. Li and H. Chen, *ACS Appl. Mater. Interfaces.*, 2020, **12**, 16700−16706.

13. Y. Zhang, C. e. Zhang, H. Huang, H. Jin, Y. Gao, R. Zheng, J. Song, C. Li, Z. Ma and Z. Bo, *Dyes Pigments.*, 2021, **184**, 108789.

14. R. Hou, M. Li, X. Ma, H. Huang, H. Lu, Q. Jia, Y. Liu, X. Xu, H. B. Li and Z. Bo, *ACS Appl. Mater. Interfaces.*, 2020, **12**, 46220−46230.

15. S. Feng, M. Li, N. Tang, X. Wang, H. Huang, G. Ran, Y. Liu, Z. Xie, W. Zhang and Z. Bo, *ACS Appl. Mater. Interfaces.*, 2020, **12**, 4638−4648.

16. S. Li, L. Zhan, F. Liu, J. Ren, M. Shi, C. Z. Li, T. P. Russell and H. Chen, *Adv. Mater.*, 2018, **30**, 1705208.

17. S. Li, L. Zhan, W. Zhao, S. Zhang, B. Ali, Z. Fu, T.-K. Lau, X. Lu, M. Shi, C.-Z. Li, J. Hou and H. Chen, *J. Mater. Chem. A.*, 2018, **6**, 12132−12141.

18. Y. Wang, Z. Liu, X. Cui, C. Wang, H. Lu, Y. Liu, Z. Fei, Z. Ma and Z. Bo, *J. Mater. Chem. A.*, 2020, **8**, 12495−12501.

19. Y. N. Chen, M. Li, Y. Wang, J. Wang, M. Zhang, Y. Zhou, J. Yang, Y. Liu, F. Liu, Z. Tang, Q. Bao and Z. Bo, *Angew.Chem. Int. Ed.*, 2020, **59**,22714−22720.

20. X. Liu, Y. Wei, X. Zhang, L. Qin, Z. Wei, H. Huang. *Sci. China Chem.*, 2020, DOI: 10.1007/s11426-020-9868-8.

21. Y. Sun, J. H. Seo, C. J. Takacs, J. Seifter and A. J. Heeger, *Adv. Mater.*, 2011, **23**,

1679−1683.

22. S. Wu, *J Adhes.*, 1973, **5**, 39−55.

23. J. Comyn, *Int J Adhesion Adhes.*, 1992, **12**, 145−149.